Plutonium Hexaboride is a Correlated Topological Insulator

Xiaoyu Deng, Kristjan Haule, and Gabriel Kotliar
Department of Physics and Astronomy, Rutgers University, Piscataway, New Jersey 08854, USA
(Received 9 August 2013; published 22 October 2013)

We predict that plutonium hexaboride (PuB_6) is a strongly correlated topological insulator, with Pu in an intermediate valence state of $Pu^{2.7+}$. Within the combination of dynamical mean field theory and density functional theory, we show that PuB_6 is an insulator in the bulk, with nontrivial Z_2 topological invariants. Its metallic surface states have a large Fermi pocket at the $\bar{X}$ point and the Dirac cones inside the bulk derived electronic states, causing a large surface thermal conductivity. PuB_6 has also a very high melting temperature; therefore, it has ideal solid state properties for a nuclear fuel material.

DOI: 10.1103/PhysRevLett.111.176404 PACS numbers: 71.20.−b, 71.28.+d, 73.20.−r

Analogies between $4f$ and $5f$ materials have proved to be a fruitful source of insights and have led to the discovery of important new classes of materials with remarkable properties. The $5f$ electrons in the actinides have substantially larger relativistic effects and the increased ionic radius of the $5f$ electrons enhances effects associated to the delocalization-localization transition. For example, the alpha to delta transition in plutonium, a $5f$ analog of the famous volume collapse transition in cerium, is the largest volume change in an elemental solid, with a volume change of the order of 30% [1]. A second noteworthy example is provided by the enhancement of the superconducting transition in 115 compounds. $PuCoGa_5$, a $5f$ analog of the Ce 115 heavy fermion superconductors, has the highest superconducting transition temperature of 18 K [2], among all the heavy fermion superconductors [3].

Motivated by the discovery of a topological insulating state [4,5] in strongly correlated samarium hexaboride (SmB_6), which has been the subject of recent interest both theoretically [6–10] and experimentally[11–22], we search for analog material among $5f$ compounds since going from $4f$'s to $5f$'s increases the f-f overlap and the resulting energy scales. We identify plutonium hexaboride (PuB_6) as a strongly correlated topological insulator at low temperatures and we investigate its physical properties using first principles methods. The theoretical information, combined with its experimentally known exceptionally high melting point [23], suggests that PuB_6 as interesting solid state properties desired for nuclear fuels.

The topological nature of an insulator, and thus the existence of topologically protected surface states, is described by topological invariants [24–28]. Most topological invariants found so far are weakly correlated band insulators [25,29,30] where topological Z_2 invariants can be found by considering all occupied bands [24–26,30–32]. For interacting systems, the proper topological invariants are defined in terms of single-particle Green's functions according to topological field theory [28,33,34]. Currently there are only a few applications to realistic materials where correlation effects are taken into account with methods beyond density functional theory, such as the local density approximation (LDA) + U and LDA + Gutzwiller method [9,35].

The LDA plus dynamical mean field theory (DMFT) method has proven a powerful framework to study the electronic structures of correlated systems [36,37]. In this Letter, we apply this method to PuB_6 and show that it is a strongly correlated topological insulator by computing the topological invariants within the DMFT framework.

The LDA + DMFT calculation is performed in the charge self-consistent implementation described in Ref. [38], which is based on the WIEN2K package [39]. We use projectors within the large (10 eV) window, and with the screening already included in this all-electron method, the Coulomb interaction is $U = 4.5$ eV, as previously determined in Ref. [40]. The other Slater integrals (F_2, F_4, and F_6) are screened even less, and are computed from the atomic physics program [41] and rescaled to 80% of their atomic value. To solve the impurity problem, we use a continuous-time quantum Monte Carlo method with hybridization expansion [42,43]. The Brillouin zone integration is performed with a regular $10 \times 10 \times 10$ mesh. The muffin-tin radius is 2.50 and 1.61 Bohr radius for Pu and B, respectively, and $R_{mt}K_{\max}$ is chosen to be 8.5 to ensure convergence.

PuB_6 is among the several binary compounds formed in plutonium-boron systems, of which most properties are still unknown [23]. It crystallizes in the same CsCl-type structure as SmB_6 with Pu at the corner and B_6 cluster at the center of the cubic unit cell, as shown in Fig. 1(a). The total density of states of PuB_6 and its projection to the plutonium atom are shown in in Fig. 2(a). The strong correlations effect is clearly visible in the distribution of the Pu-f spectra: a narrow quasiparticle peak at the Fermi level, and characteristic two peak Pu satellites, which are the quasiparticle multiplets [44] of plutonium. Because of maximum entropy method used here to analytically continue Monte Carlo data to the real axis, the satellite in the $5/2$ density of states is somewhat overbroadened, precluding the clear separation between the $5/2$ and $7/2$ satellite,

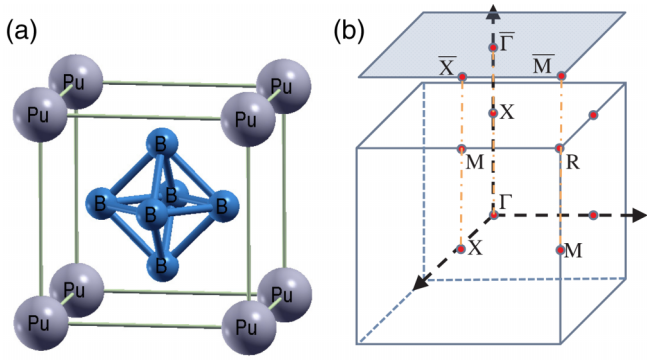

FIG. 1 (color online). (a) The crystal structure of PuB_6 with a $Pm\bar{3}m$ space group and (b) the corresponding first Brillouin zone for bulk and surface (001).

usually seen in Pu and its compounds [45,46]. To affirm the presence of these quasiparticle multiplets, we therefore also show the density of states obtained by the one-crossing approximation method [36], which is directly implemented on the real axis, and is more precise at higher frequency. The main quasiparticle peak is mainly of Pu-f-5/2 characters, and contains only a small fraction of the total spectral weight, with quasiparticle renormalization amplitude $Z = [1 - \partial\Sigma(\omega)/\partial\omega]^{-1} \simeq 0.2$. We notice a reduction

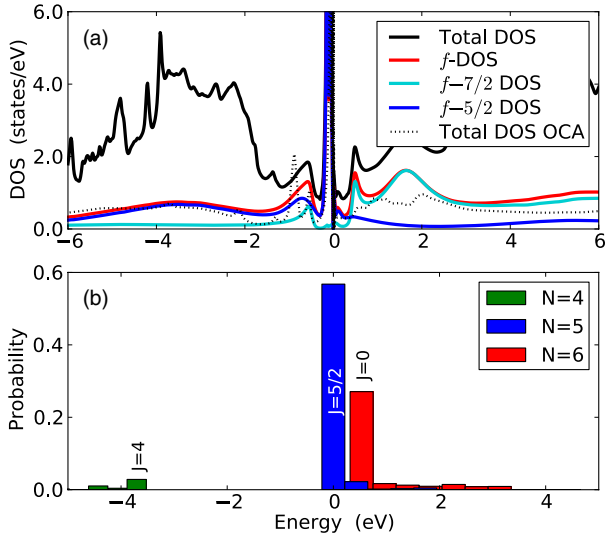

FIG. 2 (color online). The correlation signatures of PuB_6 computed with LDA + DMFT. (a) Density of states (momentum-integrated spectra) with all characters (black), the Pu-f character (red), the Pu-f-5/2-only character (blue), and the Pu-f-7/2 character (turquoise). The total density of states obtained with one-crossing approximation is shown with dots. (b) Valence histogram of PuB_6 computed by projecting the LDA + DMFT solution onto Pu atomic eigenstates. The height of the bar is the probability (percentage of time) of Pu staying on each atomic state. The x axis is the relative energy of each state to the lowest-energy atomic eigenstates. The atomic eigenstates are labeled by the total electron number N and the total angular momentum J.

of the density of states at the Fermi level indicating the formation of a small gap.

In Fig. 2(b), we show the valence histogram, which illustrates the probability of an electron on Pu to be found in any of the atomic states of the Pu atom. The probability is obtained by projecting the LDA + DMFT ground state of the solid onto the Pu atomic states, which are labeled by their quantum number $|N, J\rangle$ where N is the total electron number and J is the total angular momentum, while all the other quantum numbers are traced over. Clearly the Pu f electron is restricted mainly to $|5, 5/2\rangle$ and $|6, 0\rangle$, which highlights the strongly correlated nature of this compound. The f electron fluctuates fast between the f^5 and f^6 atomic configuration, which results in a mixed-valence nature of PuB_6, with $n_f = 5.3$. This is close, but slightly more mixed valent than the elemental Pu [40]. The mixed-valent nature suggests a strong screening of the magnetic moments; therefore, we expect that PuB_6 has a nonmagnetic ground state, in agreement with the theoretical calculation.

The momentum-resolved spectra $A(k, \omega)$ is shown in Fig. 3(a). Nearly flat quasiparticle bands are located at the Fermi level with an overall bandwidth of about 0.15 eV, and lighter bands further away from the Fermi level. Consistent with the density of states, the quasiparticle bands have mainly f-5/2 characters and the spectra of the f-7/2 character is pushed away from the Fermi level. A broad band, which is mainly of a Pu-d character, crosses all f-derived states in the vicinity of the $X(\pi, 0, 0)$ point,

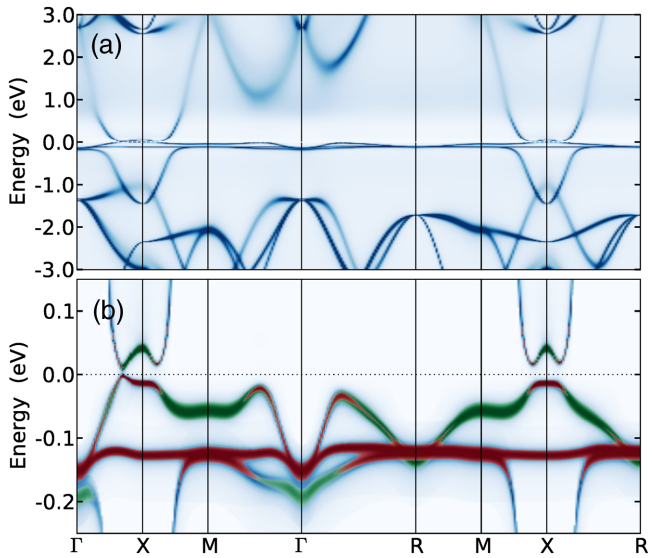

FIG. 3 (color online). The momentum-resolved spectra of PuB_6 computed within the LDA + DMFT method in a broad energy range (a), and a corresponding zoom in around Fermi level (b) where we also depict different character of f orbitals. Spectra with the Pu-f-Γ_8^- character and the Pu-f-Γ_7^- character are indicated by red and green, respectively. The corresponding basis functions are $\Gamma_8^{(1)} = \sqrt{\frac{5}{6}}|\pm\frac{5}{2}\rangle + \sqrt{\frac{1}{6}}|\mp\frac{3}{2}\rangle$, $\Gamma_8^{(2)} = |\pm\frac{1}{2}\rangle$ for the Γ_8^- quartet and $\Gamma_7 = \sqrt{\frac{1}{6}}|\pm\frac{5}{2}\rangle - \sqrt{\frac{5}{6}}|\mp\frac{3}{2}\rangle$ for the Γ_7^- doublet.

resulting in a band inversion between d orbitals and f orbitals. This band inversion implies a charge transfer from Pu f orbitals to Pu d orbitals and is consistent with the mixed-valent nature revealed in the valence histogram. By examining the detailed structure of the quasiparticle bands near the Fermi level [Fig. 3(b)], we find clearly that a small gap opens in the vicinity of the X point, making PuB_6 a narrow gap semiconductor. In cubic lattice environment, the f-5/2 orbitals are split into two levels: a quartet with Γ_8^- symmetry and a doublet with Γ_7^- symmetry. The orbital character is depicted in Fig. 3(b). We see that both Γ_8^- and Γ_7^- states substantially contribute to the bands near Fermi level, and both have to be taken into account in modeling this compound.

We also check the LDA band structure of PuB_6 for comparison, as shown in Fig. 4. We note that LDA also predicts the insulating state for PuB_6. The main differences between the two theoretical methods is that the f-derived states are much broader within LDA (about 0.5 eV compared to 0.15 eV in DMFT), and the f-7/2 states are centered just above the Fermi level in LDA, in contrast to LDA + DMFT. Despite these differences, the low energy gap structure of the two methods is quite similar near the Fermi level, with only slightly larger gap in LDA, and a direct gap in LDA + DMFT and slightly indirect in LDA. Notice also that the high frequency spectra of mostly light bands (below -1 eV and above 2 eV) are very similar in both methods.

After establishing the fact that PuB_6 is a correlated mixed-valent insulator, we turn to its topological nature. To compute the topological invariant of an interaction system, we follow Ref. [28]. Here the self-energy has no singularity in the vicinity of the Fermi level; hence, only the Green's function at zero frequency $G^{-1}(k,0) = \mu - H(k) - \Sigma(k,0)$ is needed to determine the topology of the quasiparticle states. Following Refs. [33,47], we hence compute the topological invariant for a noninteracting Hamiltonian defined by $H_t(k) = H(k) + \Sigma(k,0) - \mu$. Owing to the inversion symmetry of PuB_6, we only need to compute the parities of all occupied states on the time reversal invariant momenta (TRIM) points [24,25,31]. This method can be applied to the LDA + DMFT calculation, which is the same as the approaches used in slave-boson, LDA + Gutzwiller, and LDA + U studies [7–10,35]. In PuB_6 there are four independent TRIMs: $\Gamma(0,0,0)$, $X(0,0,\pi)$, $M(0,\pi,\pi)$, $R(\pi,\pi,\pi)$. Following the above technique the counted parity products of TRIMs are presented in Table I. This is consistent with the naive observation that there is a band inversion of d orbitals and f orbitals at the X point which contributes a parity change of -1, while for the other TRIM points, there is no band inversion. The Z_2 topological index is (1:111). We conclude that PuB_6 is a strong topological insulator in the prediction of the LDA + DMFT method and it belongs to the same topological class as SmB_6 [9].

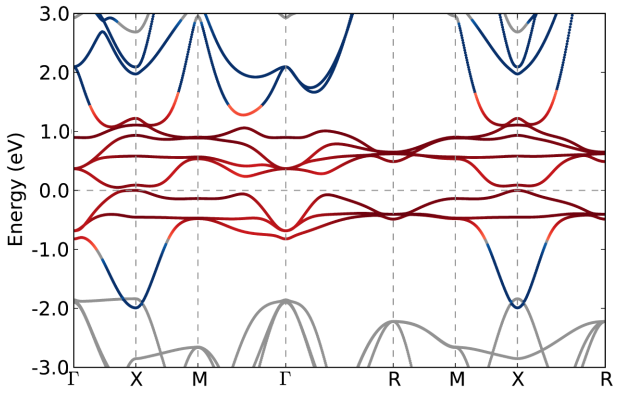

FIG. 4 (color online). The band structure of PuB_6 computed by LDA. The relative weight of the Pu-f character and d bands is labeled by colors: red is mainly the f character and and blue is mainly the d character. Other characters are indicated by gray.

Topologically protected surface states emerge as a consequence of the nontrivial topological nature of the bulk system. To study the surface states, we first construct the tight-binding Hamiltonian $H(k)$ from the LDA calculation using the maximally localized Wannier functions [48–50]. At low energy, the computed self-energy can be approximated by a Fermi-liquid-like form $\Sigma(k,\omega) \approx \Sigma_k(0) + (1 - 1/Z_k)\omega$ (the imaginary part is ignored), which leads to an effective topological Hamiltonian

$$H_t^{\text{eff}} = \sqrt{Z_k}[H(k) + \Sigma_k(0) - \mu_f]\sqrt{Z_k},$$

where $\sqrt{Z}$ and $\Sigma(0)$ are diagonal matrices in orbital space, vanishing on the Pu-d orbital. It has the same parities at the TRIMs as the topological Hamiltonian $H_t = H(k) + \Sigma_k(0) - \mu_f$ [47]. This is a quasiparticle Hamiltonian, which accurately reproduces the quasiparticle bands at low frequency. We then expect that the surface states of quasiparticles can be captured by this effective topological Hamiltonian. We solve the tight-binding model on a slab constructed with this Hamiltonian to get the surface states on the (001) surface. As shown in Fig. 5(a), we find that gapless edge states show up in the bulk gap around $\bar{\Gamma}$ and $\bar{X}$, which is consistent with the nontrivial topological invariants. In our results the Dirac point at $\bar{X}$ is deep inside the bulk states, and consequently the Fermi surface at $\bar{X}$ point is large.

Recent studies postulate minimum model Hamiltonians for such d-f hybridization system were based on the assumption that crystal field splitting are large enough

TABLE I. The product of parities eigenvalues computed from the occupied states of the topological Hamiltonians at eight TRIMs in the Brillouin zone.

Γ	$3X$	$3M$	R
$+1$	-1	$+1$	$+1$

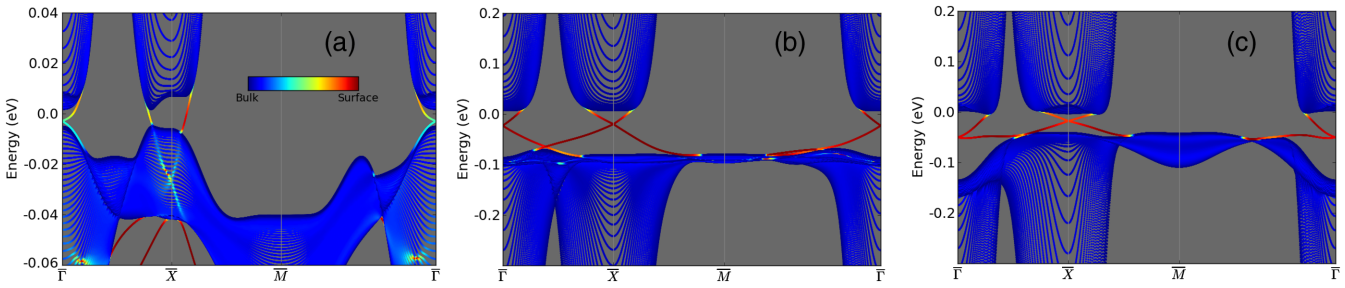

FIG. 5 (color online). Surface states of PuB_6 on the (001) surface. The band structure is calculated with a tight-binding model for a 60-layer slab constructed from the effective topological Hamiltonian including Pu-d-e_g orbitals and Pu-f orbitals (a). The weight of the surface state (the probability of each state in the first two layers on surface) is indicated by color: red means more weight on the surface, blue means more weight in the bulk. The same calculation is done with an effective model Hamiltonian in which only f-Γ_8^- orbitals or only f-Γ_7^- orbitals are included in addition to d-e_g orbitals, and the corresponding surface states are shown in (b) and (c), respectively.

that only one crystal level of f orbitals is relevant [6,10,35]. To understand the effects of such artificial enhancement of the crystal field splitting on the surface states, we construct two alternative low energy models, keeping either Γ_8^- or Γ_7^- states only. The corresponding surface states are shown in Figs. 5(b) and 5(c). In both models we obtain much larger gaps. There are gapless edge states in agreement with previous model calculations, although the detailed dispersion of edge states are somewhat different due to details in the hopping parameters. Three Dirac cones show up in the gap at $\bar{X}$ and $\bar{\Gamma}$ in consistent with previous reports [9,10]. Therefore we conclude that while the existence of gapless edge states is protected by the topology, the details of the edge states depend sensitively on the chosen crystal field splittings in model Hamiltonians.

Recently SmB_6, which within the LDA + DMFT method is similar to PuB_6, has been studied intensively to understand the interplay of correlation effects with topology, and it was argued to be a model topological Kondo insulator [7–10]. It has also been argued that SmB_6 is an ideal topological insulator in which the conductance is dominated by surface states at a low temperature [12,14,19]. Our prediction of PuB_6 with similar topological properties provides an alternative to these intriguing studies, and may promote more experimental investigations and theoretical understandings. In particular, the larger energy scales associated with a $5f$ material should result in a more clear picture of the surface bulk correspondence. PuB_6 is not only of high scientific importance but may also have solid state properties important for technological applications. The relatively small hybridization gap and more importantly the topologically protected metallic surface states of PuB_6 with large Fermi surface pockets, should result in an exceptionally high thermal conductivity for an insulating materials. PuB_6 has also a very high melting point, approximately 2200 K. These are ideal solid state properties for a nuclear fuel. Since B is a standard moderator in use in nuclear reactors, PuB_6 might be a model system in which to explore the properties of topological nuclear fuels.

We acknowledge very useful discussions with S. Savrasov, X. Dai, J. Z. Zhao, Z. P. Yin, and N. Lanata. X. D. and G. K. are supported by BES-DOE Grant No. DE-FG02-99ER45761; K. H. is supported by the NSF DMR 0746395.

[1] S. S. Hecker and L. F. Timofeeva, Los Alamos Sci. **26**, 244 (2000).
[2] J. L. Sarrao, L. A. Morales, J. D. Thompson, B. L. Scott, G. R. Stewart, F. Wastin, J. Rebizant, P. Boulet, E. Colineau, and G. H. Lander, Nature (London) **420**, 297 (2002).
[3] J. L. Sarrao and J. D. Thompson, J. Phys. Soc. Jpn. **76**, 051013 (2007).
[4] X.-L. Qi and S.-C. Zhang, Rev. Mod. Phys. **83**, 1057 (2011).
[5] M. Z. Hasan and C. L. Kane, Rev. Mod. Phys. **82**, 3045 (2010).
[6] T. Takimoto, J. Phys. Soc. Jpn. **80**, 123710 (2011).
[7] M. Dzero, K. Sun, V. Galitski, and P. Coleman, Phys. Rev. Lett. **104**, 106408 (2010).
[8] M. Dzero, K. Sun, P. Coleman, and V. Galitski, Phys. Rev. B **85**, 045130 (2012).
[9] F. Lu, J. Z. Zhao, H. Weng, Z. Fang, and X. Dai, Phys. Rev. Lett. **110**, 096401 (2013).
[10] V. Alexandrov, M. Dzero, and P. Coleman, arXiv:1303.7224.
[11] H. Miyazaki, T. Hajiri, T. Ito, S. Kunii, and S. I. Kimura, Phys. Rev. B **86**, 075105 (2012).
[12] S. Wolgast, C. Kurdak, K. Sun, J. W. Allen, D.-J. Kim, and Z. Fisk, arXiv:1211.5104.
[13] X. Zhang, N. P. Butch, P. Syers, S. Ziemak, R. L. Greene, and J. Paglione, Phys. Rev. X **3**, 011011 (2013).
[14] D. J. Kim, S. Thomas, T. Grant, J. Botimer, Z. Fisk, and J. Xia, arXiv:1211.6769.
[15] N. Xu, X. Shi, P. K. Biswas, C. E. Matt, R. S. Dhaka, Y. Huang, N. C. Plumb, M. Radovic, J. H. Dil, E. Pomjakushina, A. Amato, Z. Salman, D. M. Paul, J. Mesot, H. Ding, and M. Shi, Phys. Rev. B **88**, 121102(R) (2013).

[16] M. Neupane, N. Alidoust, S.-Y. Xu, T. Kondo, D.-J. Kim, C. Liu, I. Belopolski, T.-R. Chang, H.-T. Jeng, T. Durakiewicz, L. Balicas, H. Lin, A. Bansil, S. Shin, Z. Fisk, and M. Z. Hasan, arXiv:1306.4634.
[17] G. Li, Z. Xiang, F. Yu, T. Asaba, B. Lawson, P. Cai, C. Tinsman, A. Berkley, S. Wolgast, Y. S. Eo, D.-J. Kim, C. Kurdak, J. W. Allen, K. Sun, X. H. Chen, Y. Y. Wang, Z. Fisk, and L. Li, arXiv:1306.5221.
[18] J. Jiang, S. Li, T. Zhang, Z. Sun, F. Chen, Z. R. Ye, M. Xu, Q. Q. Ge, S. Y. Tan, X. H. Niu, M. Xia, B. P. Xie, Y. F. Li, X. H. Chen, H. H. Wen, and D. L. Feng, arXiv:1306.5664.
[19] D. J. Kim, J. Xia, and Z. Fisk, arXiv:1307.0448.
[20] S. Thomas, D. J. Kim, S. B. Chung, T. Grant, Z. Fisk, and J. Xia, arXiv:1307.4133.
[21] E. Frantzeskakis, N. de Jong, B. Zwartsenberg, Y. K. Huang, Y. Pan, X. Zhang, J. X. Zhang, F. X. Zhang, L. H. Bao, O. Tegus, A. Varykhalov, A. de Visser, and M. S. Golden, arXiv:1308.0151.
[22] M. M. Yee, Y. He, A. Soumyanarayanan, D.-J. Kim, Z. Fisk, and J. E. Hoffman, arXiv:1308.1085.
[23] P. Rogl and P. Potter, J. Phase Equilib. **18**, 467 (1997).
[24] C. L. Kane and E. J. Mele, Phys. Rev. Lett. **95**, 146802 (2005).
[25] L. Fu and C. L. Kane, Phys. Rev. B **76**, 045302 (2007).
[26] J. E. Moore and L. Balents, Phys. Rev. B **75**, 121306 (2007).
[27] X.-L. Qi, T. L. Hughes, and S.-C. Zhang, Phys. Rev. B **78**, 195424 (2008).
[28] Z. Wang and S.-C. Zhang, Phys. Rev. X **2**, 031008 (2012).
[29] B. A. Bernevig, T. L. Hughes, and S.-C. Zhang, Science **314**, 1757 (2006).
[30] H. Zhang, C.-X. Liu, X.-L. Qi, X. Dai, Z. Fang, and S.-C. Zhang, Nat. Phys. **5**, 438 (2009).
[31] L. Fu, C. L. Kane, and E. J. Mele, Phys. Rev. Lett. **98**, 106803 (2007).
[32] H. Zhang and S.-C. Zhang, Phys. Status Solidi RRL **7**, 72 (2013).
[33] Z. Wang, X.-L. Qi, and S.-C. Zhang, Phys. Rev. B **85**, 165126 (2012).
[34] X.-L. Qi, R. Li, J. Zang, and S.-C. Zhang, Science **323**, 1184 (2009).
[35] X. Zhang, H. Zhang, J. Wang, C. Felser, and S.-C. Zhang, Science **335**, 1464 (2012).
[36] G. Kotliar, S. Y. Savrasov, K. Haule, V. S. Oudovenko, O. Parcollet, and C. A. Marianetti, Rev. Mod. Phys. **78**, 865 (2006).
[37] K. Held, Adv. Phys. **56**, 829 (2007).
[38] K. Haule, C.-H. Yee, and K. Kim, Phys. Rev. B **81**, 195107 (2010).
[39] P. Blaha, K. Schwarz, G. K. H. Madsen, D. Kvasnicka, and J. Luitz, *WIEN2K, An Augmented Plane Wave + Local Orbitals Program for Calculating Crystal Properties* (Karlheinz Schwarz, Techn. Universität Wien, Austria, 2001).
[40] J. H. Shim, K. Haule, and G. Kotliar, Nature (London) **446**, 513 (2007).
[41] R. D. Cowan, *The Theory of Atomic Structure and Spectra* (University of California Press, Berkeley, 1981).
[42] K. Haule, Phys. Rev. B **75**, 155113 (2007).
[43] P. Werner, A. Comanac, L. de' Medici, M. Troyer, and A. J. Millis, Phys. Rev. Lett. **97**, 076405 (2006).
[44] C.-H. Yee, G. Kotliar, and K. Haule, Phys. Rev. B **81**, 035105 (2010).
[45] T. Gouder, F. Wastin, J. Rebizant, and L. Havela, Phys. Rev. Lett. **84**, 3378 (2000).
[46] T. Durakiewicz, J. J. Joyce, G. H. Lander, C. G. Olson, M. T. Butterfield, E. Guziewicz, A. J. Arko, L. Morales, J. Rebizant, K. Mattenberger, and O. Vogt, Phys. Rev. B **70**, 205103 (2004).
[47] Z. Wang and B. Yan, J. Phys. Condens. Matter **25**, 155601 (2013).
[48] A. A. Mostofi, J. R. Yates, Y.-S. Lee, I. Souza, D. Vanderbilt, and N. Marzari, Comput. Phys. Commun. **178**, 685 (2008).
[49] J. Kuneš, R. Arita, P. Wissgott, A. Toschi, H. Ikeda, and K. Held, Comput. Phys. Commun. **181**, 1888 (2010).
[50] N. Marzari, A. A. Mostofi, J. R. Yates, I. Souza, and D. Vanderbilt, Rev. Mod. Phys. **84**, 1419 (2012).